

Article

The Influence of pH on the Combustion Properties of Bio-Coal Following Hydrothermal Treatment of Swine Manure

Aidan Mark Smith ^{1,*} , Ugochinyere Ekpo ² and Andrew Barry Ross ²

¹ School of Biological and Chemical Engineering, Aarhus University, 8200 Aarhus, Denmark

² School of Chemical and Process Engineering, University of Leeds, Leeds LS2 9JT, UK; cn10une@leeds.ac.uk (U.E.); a.b.ross@leeds.ac.uk (A.B.R.)

* Correspondence: aidan.smith@eng.au.dk; Tel.: +45-93-52-12-15

Received: 29 November 2019; Accepted: 6 January 2020; Published: 9 January 2020



Abstract: The application of excessive amounts of manure to soil prompted interest in using alternative approaches for treating slurry. One promising technology is hydrothermal carbonisation (HTC) which can recover nutrients such as phosphorus and nitrogen while simultaneously making a solid fuel. Processing manure under acidic conditions can facilitate nutrient recovery; however, very few studies considered the implications of operating at low pH on the combustion properties of the resulting bio-coal. In this work, swine manure was hydrothermally treated at temperatures ranging from 120 to 250 °C in either water alone or reagents including 0.1 M NaOH, 0.1 M H₂SO₄, and finally 0.1 M organic acid (CH₃COOH and HCOOH). The influence of pH on the HTC process and the combustion properties of the resulting bio-coals was assessed. The results indicate that pH has a strong influence on ash chemistry, with decreasing pH resulting in an increased removal of ash. The reduction in mineral matter influences the volatile content of the bio-coal and its energy content. As the ash content in the final bio-coal reduces, the energy density increases. Treatment at 250 °C results in a more “coal like” bio-coal with fuel properties similar to that of lignite coal and a higher heating value (HHV) ranging between 21 and 23 MJ/kg depending on pH. Processing at low pH results in favourable ash chemistry in terms of slagging and fouling. Operating at low pH also appears to influence the level of dehydration during HTC. The level of dehydration increases with decreasing pH, although this effect is reduced at higher temperatures. At higher-temperature processing (250 °C), operating at lower pH increases the yield of bio-coal; however, at lower temperatures (below 200 °C), the reverse is true. The lower yields obtained below 200 °C in the presence of acid may be due to acid hydrolysis of carbohydrate in the manure, whereas, at the higher temperatures, it may be due to the acid promoting polymerisation.

Keywords: HTC; bio-coal; manure; slagging; fouling; corrosion; process chemistry; combustion; waste to energy

1. Introduction

Historically, animal manures were returned to land and used in agriculture to increase soil organic matter and provide plant nutrients. The expansion of concentrated animal husbandry over the latter half of the 20th century, however, resulted in thousands of animals often being concentrated into small geographical areas, overwhelming the nutrient needs and soil-absorbing capacity of the nearby land. Excessive nutrients can then leach into groundwater, potentially leading to surface and groundwater pollution. As such, disposal of animal manures is a problem [1]. Hydrothermal treatment, including hydrothermal carbonisation (HTC), is an emerging technology which is well suited to processing wet

wastes such as manure, and it has potential for recovery of nutrients from biomass and wastes such as phosphorus and nitrogen while simultaneously producing a solid fuel for energetic purposes [2].

Hydrothermal treatment involves the processing of biomass in water at temperatures above 100 °C at elevated pressure to ensure the water is in the liquid phase. HTC typically uses a temperature range of 180 to 250 °C, while temperatures below 180 °C are typically regarded as thermal hydrolysis. Under hydrothermal conditions, water acts as both reagent and medium for a series of aqueous and solid-phase reactions to take place, leading to the carbonisation of biomass, resulting in a hydrochar or bio-coal, which has similar properties to a low-rank coal. [3]. Animal manures are typically composed of faeces, urine, discarded bedding, and waste feed. They have high moisture content, and they are, therefore, well suited for conversion by HTC [1]. During the hydrothermal processing of plant biomass, a number of key plant nutrients, including potassium and phosphorus from soluble phosphates, can be extracted into the aqueous phase and subsequently precipitated and recovered [4,5]. The extent to which the phosphorus is extracted is feedstock-dependent, with the inorganic content of the feedstock, particularly calcium content, often a key variable [6].

Previous studies investigating the HTC of manures found that phosphorus within manures is not easily extracted, leading to the immobilisation of the phosphorus in the bio-coal. This prompted the application of acids in HTC to aid phosphorus extraction [2,7,8]. The addition of acids during HTC was widely investigated, and it is thought to improve the overall rate of reaction in HTC [9–13]. In a study reported by Reza et al. [14], the influence of feedwater pH on the HTC of wheat straw was investigated using acetic acid and potassium hydroxide. The results indicated that the feedwater pH influences carbon density and higher heating value (HHV) in wheat straw, with higher carbon densities associated with lower pH.

At present, the application of acid catalysis for the processing of manures is primarily focused on increasing the extraction of phosphorus. Ekpo et al. [8] and Dai et al. [7] investigated the influence of acids on the recovery of phosphorus and nitrogen in swine and cattle manures, respectively. Ekpo et al. [8] investigated the addition of sodium hydroxide, sulphuric acid, acetic acid, and formic acid at 0.1 molar concentration and demonstrated that the presence of acidic additives improves the extraction of phosphorus and nitrogen. This study showed that phosphorus extraction is pH- and temperature-dependent and enhanced under acidic conditions. Phosphorus was most readily extracted using sulphuric acid, reaching 94% at 170 °C, while largely retained in the residue for all other conditions [8]. Dai et al. [7] performed HTC at 190 °C for 12 h using hydrochloric acid at varying concentrations. The results indicated that HTC in 2% hydrochloric acid extracted almost 100% phosphorus and 63% nitrogen. Decreasing the pH results in a small increase in carbon content and a large decrease in oxygen content, which will increase energy content (not stated). Decreasing the pH, however, also impacts the yields of bio-coal, which reduces from 70% (db) to 53% (db), and this reduction appears to be predominantly associated with the removal of oxygen. Fuel volatile matter is also seen to decrease, corresponding to an increase in fixed carbon at low pH. Ghanim et al. [15] investigated the HTC of poultry litter at 250 °C for 2 h at different pH using acetic and sulphuric acid. Once again, the results indicate that operation at low pH increases the carbon content and HHV of the bio-coal. Increasing sulphuric acid content appears to both increase yield of bio-coal and reduce ash content. These results suggest that performing HTC in dilute acid can simultaneously facilitate nutrient recovery from manure while upgrading the manure to a higher-quality bio-coal.

The studies performed to date did not consider the implications of operating at low pH on the inorganic chemistry, and how this affects the combustion behaviour of the bio-coal. The presence of inorganics and heteroatoms is a particular issue during thermochemical conversion of biomass and feedstocks that contain large amounts of potassium, sodium, sulphur, and chlorine; it can result in corrosion and slagging, or fouling in furnace and retorts [16]. Slagging is a process that occurs when ash deposits melt due to exposure to radiant heat, such as flames in a furnace. As this ash begins to melt, it starts to fuse, becomes sticky, and eventually forms a hard glassy slag known as a clinker, making ash removal difficult. A high ash melting temperature is desirable as most furnaces are designed to

remove ash as a powdery residue [16]. Fouling occurs when potassium and sodium chlorides within the fuel partially evaporate on exposure to radiant heat and then condense on cooler surfaces such as heat exchangers forming alkali chloride deposits, which reduces their efficiency on heat exchangers. These alkali chlorides can also play a role in the corrosion as they can react with sulphur in the flue gas, forming alkali sulphates and liberating chlorine within the deposit. This chlorine then catalyses the active oxidation and corrosion of the steel on which the deposit is formed [16,17].

To reduce the chance of a fuel slagging or fouling, it is important to minimise the alkali metal content in the ash along with chlorine. Leaching of alkaline metals and chlorine during HTC was demonstrated in a number of studies that concluded that slagging, fouling, and corrosion can be reduced by reducing alkali metals [18–24]. This reduction in slagging and fouling propensity following HTC was first demonstrated by Reza et al. [25] and later developed by Smith et al. [26], who demonstrated the effect of alkali metal removal on ash melting temperatures for HTC bio-coal using ash fusion analysis. This was later validated by subsequent studies [27–30].

The work presented in Smith et al. [26], however, demonstrated that the reduction in slagging and fouling propensity of HTC bio-coal is only partially due to a reduction of alkali metals, and it is also influenced by the retention of calcium and phosphorus within the bio-coal. Calcium and phosphorus are important as, while alkali metals, such as potassium and sodium, act as a flux for alumina–silicate ash, alkaline earth metals, such as calcium and magnesium, tend to increase melting temperatures [16]. In addition to the alkali and alkaline earth metals, the presence of phosphorus can prevent alkali metals forming low-melting-temperature alkali silicates, instead forming thermally stable phosphate compounds [31]. Phosphorus is also important from a fouling perspective, as potassium and sodium chlorides present within the ash can bind with calcium-rich phosphates to produce potassium or sodium phosphates, which then further react with calcium oxides. The resulting calcium potassium phosphate/calcium sodium phosphate complexes are stable and remove the potassium/sodium available to form low-melting-temperature potassium silicates [31,32]. Calcium oxide, calcium carbonate, and calcium hydroxide would otherwise dissolve into potassium/sodium silicate melts, bringing about the release of the potassium or sodium into the gas phase [33,34]. The removal of inorganics by the addition of acids during HTC may have a profound effect on the ash chemistry and affect the properties of the bio-coal during subsequent thermochemical processing.

In this work, swine manure was hydrothermally treated between 120 and 250 °C in water or 0.1 M NaOH, 0.1 M H₂SO₄, or 0.1 M organic acid (CH₃COOH and HCOOH). The influence of pH on the on the HTC process was assessed, and the combustion properties of the resulting fuels were assessed.

2. Materials and Methods

2.1. Materials

The swine manure was collected from the University of Leeds farm. Prior to processing and characterisation, the manure was dried in an oven at 60 °C for several days and homogenised in an Agate Tema barrel.

2.2. Hydrothermal Processing

Hydrothermal processing of the swine manure was performed in an unstirred 600-mL Parr reactor (Parr, Moline, IL, USA). For each experiment, the reactor was filled with 24 g of swine manure and either 220 mL of de-ionised water (pH ≈ 6) or solutions of 0.1 M NaOH, 0.1 M H₂SO₄ (pH 13 and 1, respectively), or 0.1 M organic acid (CH₃COOH and HCOOH) (pH 2.88 and 2.38, respectively) to form a slurry. Hydrothermal processing was performed at 120 °C, 170 °C, 200 °C, and 250 °C for 1 h. The heating rate was approximately 10 °C·min⁻¹, and the residence time was taken from when the reactor reached the desired temperature. After one hour, the reactor was removed from the heating jacket and then allowed to cool to room temperature before the products were separated.

Bio-coal samples were dried in an oven at 60 °C for a minimum of 24 h, and yields were taken as dry bio-coal mass compared with the original dry mass of unprocessed manure.

2.3. Analysis

2.3.1. Inorganic Analysis

For analysis, dried samples were ground and homogenised to below 100 µm. Samples were ashed in a muffle furnace (Nabertherm, Lilienthal, Germany) to a final temperature of 550 °C, with a hold at 250 °C to minimise volatile metal loss, as directed in BS EN ISO 18122-2. The ash was then mixed with a lithowax binder at a 10:1 ratio and palletised using a laboratory press (Spex, Stanmore, UK). The elemental composition of the ash was then determined using wavelength-dispersive X-ray fluorescence (WD-XRF) (Rigaku, Tokyo, Japan) using a metal oxide method. To correct for residual carbon within the ash, the carbon content was determined using a CHNS analyser (Thermo Scientific, Waltham, MA, USA), and carbon content was manually input to the XRF component list.

2.3.2. Organic Analysis and Determination of Combustion Properties

The carbon, hydrogen, nitrogen, and oxygen contents were determined using a Flash 2000 CHNS-0 analyser (Thermo Scientific, Waltham, MA, USA), calibrated using both chemical standards and certified biomass reference materials (Elemental Microanalysis, Okehampton, UK). Hydrogen and oxygen values were corrected to account for residual moisture, and figures are given on a dry free basis, in accordance with ASTM D3180-15. The error stated is based on the calculated standard error. The higher heating value (HHV) was calculated by bomb calorimetry (Parr, Moline, IL, USA). Proximate analysis was undertaken using a thermogravimetric analyser (TGA) (Mettler Toledo, Columbus, OH, USA). To obtain the residual moisture, 10 µg of homogenised sample was heated under nitrogen to 105 °C, where the temperature was held for 10 min before heating at 25 °C·min⁻¹ to 900 °C to determine the volatile carbon content. Fixed carbon was determined by holding the temperature at 900 °C and switching to air. Burning profiles, ignition, flame stability, and burnout temperature were obtained by temperature-programmed oxidation (TPO) in a TGA (Mettler Toledo, Columbus, OH, USA). Then, 10 µg of homogenised sample was heated at a rate of 10 °C·min⁻¹ in air to 900 °C, and the first derivative of the weight loss was calculated.

2.3.3. Prediction of Slagging and Fouling Propensity

The propensity of the fuels to slag and foul was assessed using both predictive slagging and fouling indices in the ash fusion test (AFT). Slagging and fouling indices are numerical indices based on the ash composition, as determined in Section 2.3.1. The equations for the alkali index (AI), bed agglomeration index (BAI), and acid base ratio (R_a^b) are given in Table 1, along with the key values indicative of the onset of issues. The AFT is a qualitative method of assessing the propensity of a fuel to slag, and it works by heating an ash test piece and analysing the transitions in the ash chemistry in accordance with DD CEN/TS 15370-1:2006. Cylindrical test pieces are formed using 550 °C ash and a dextrin binder (Sigma-Aldrich, USA). The sample is then heated from 550 °C to 1570 °C in an ash fusion furnace (Carbolite, UK) using an airflow of 50 mL·min⁻¹ to give an oxidising atmosphere. The key transitions are as follows: (i) shrinkage, which predominantly represents the decomposition of carbonates in hydrothermally derived chars, (ii) deformation temperature, essentially representing the onset point at which the powdery ash starts to agglomerate and starts to stick to surfaces, (iii) hemisphere, whereby ash is agglomerating and is sticky, and (v) flow, whereby the ash melts [29]. The temperature for each transition is given to the nearest 10 °C in accordance with the standard. For most power stations, slagging becomes problematic between the deformation and hemisphere temperature [29]; thus, the deformation temperature is taken as the onset temperature for slag related issues.

Table 1. Predictive slagging and fouling indices.

Slagging/Fouling Index	Expression	Limit	
Alkali Index (AI)	$AI = \frac{Kg (K_2O + Na_2O)}{GJ}$	AI < 0.17, safe combustion AI > 0.17 < 0.34, probable slagging and fouling AI > 0.34, almost certain slagging and fouling [35]	Equation (1)
Bed Agglomeration Index (BAI)	$BAI = \frac{\%(Fe_2O_3)}{\%(K_2O + Na_2O)}$	BAI < 0.15, bed agglomeration likely [36]	Equation (2)
Acid Base Ratio (R_a^b)	$R_a^b = \frac{\%(Fe_2O_3 + CaO + MgO + K_2O + Na_2O)}{\%(SiO_2 + TiO_2 + Al_2O_3)}$	$R_a^b < 0.5$, low slagging risk [36]	Equation (3)

3. Results

3.1. Influence of pH on Bio-Coal Composition

The yields and ultimate analysis of the bio-coals derived from the swine manure are given in Table 2. The results show that, with decreasing pH, there is increased removal of ash, with lower-pH treatments having the lowest ash content for their respective temperature. The exception is acetic acid (pH 2.88), which appears to have slightly lower ash content than formic acid (pH 2.38). Yields on a dry basis also appear to be influenced by pH, with higher yields associated with lower pH. The exception to this is sulphuric acid at lower temperatures, with lower yields observed at 120 °C than that for the higher-pH treatments. This lower yield is in part because of the reduced ash content; however, the reduction in ash alone does not account for the reduced yield, and the results suggest that the lower yields appear to be due to enhanced oxygen removal. Due to the variation between ash contents with differing pH, Table 3 gives the ultimate analysis on a dry ash free (daf) basis, to enable direct comparisons between the organic chemistry of the different treatments. The results show that, for the 120 °C treatment in sulphuric acid, there is a higher carbon density and lower oxygen content for this treatment than the higher-pH treatments at this temperature.

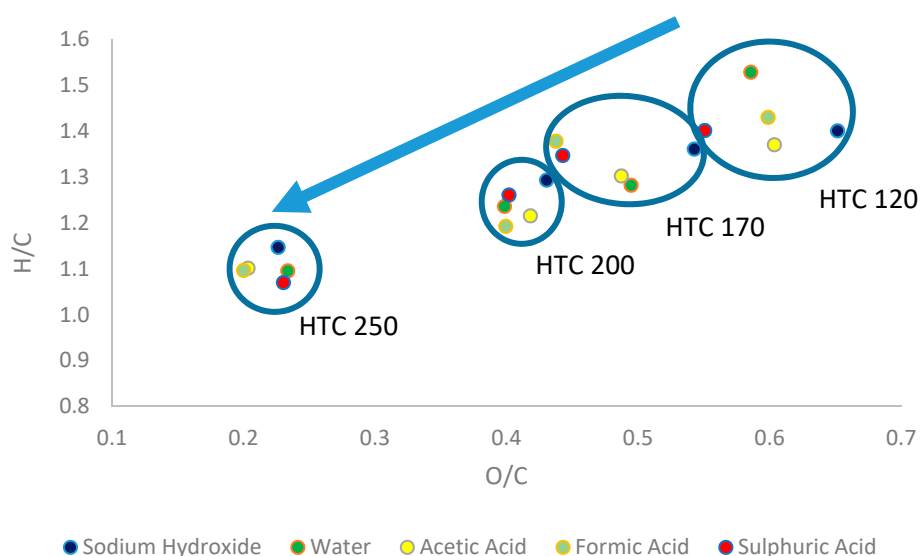
Table 2. Ultimate analysis and yields of fuels on a dry basis; n/a—not applicable.

Sample Name	Dry Basis						Ash (wt.%)
	Yield (%)	C (wt.%)	H (wt.%)	N (wt.%)	S (wt.%)	O (wt.%)	
Unprocessed Pig Manure	n/a	44.0 ± 0.5	5.1 ± 0.1	2.9 ± 0.1	0.2 ± 0.0	35.7 ± 0.7	12.6
Sodium Hydroxide 120 °C	84	42.7 ± 0.3	5.0 ± 0.0	2.4 ± 0.0	0.1 ± 0.0	37.1 ± 0.5	12.6
Sodium Hydroxide 170 °C	64	45.0 ± 0.2	5.1 ± 0.1	2.1 ± 0.0	0.1 ± 0.0	32.6 ± 0.9	15.2
Sodium Hydroxide 200 °C	59	48.4 ± 0.2	5.2 ± 0.1	2.4 ± 0.0	0.2 ± 0.0	27.8 ± 0.0	16.0
Sodium Hydroxide 250 °C	41	49.8 ± 0.0	4.8 ± 0.0	2.5 ± 0.0	0.3 ± 0.0	15.0 ± 0.1	27.6
Water 120 °C	86	45.4 ± 0.5	5.8 ± 0.4	2.4 ± 0.1	0.1 ± 0.0	35.5 ± 1.0	10.7
Water 170 °C	62	47.3 ± 0.3	5.0 ± 0.0	2.3 ± 0.1	0.2 ± 0.0	31.2 ± 0.4	14.0
Water 200 °C	59	50.8 ± 0.3	5.2 ± 0.0	2.4 ± 0.0	0.2 ± 0.0	27.0 ± 0.1	14.3
Water 250 °C	43	53.5 ± 3.4	4.9 ± 0.4	2.8 ± 0.2	0.3 ± 0.0	16.7 ± 0.3	21.9
Acetic Acid 120 °C	83	45.0 ± 0.2	5.1 ± 0.0	2.6 ± 0.1	0.1 ± 0.0	36.2 ± 0.4	11.0
Acetic Acid 170 °C	61	47.9 ± 0.7	5.2 ± 0.1	2.5 ± 0.1	0.1 ± 0.0	31.1 ± 0.6	13.0
Acetic Acid 200 °C	59	50.1 ± 0.8	5.1 ± 0.1	2.3 ± 0.1	0.1 ± 0.0	27.9 ± 1.9	14.5
Acetic Acid 250 °C	44	56.6 ± 0.6	5.2 ± 0.1	2.9 ± 0.0	0.2 ± 0.0	15.4 ± 0.1	19.7
Formic Acid 120 °C	83	45.0 ± 1.1	5.4 ± 0.2	2.5 ± 0.1	0.2 ± 0.0	35.9 ± 1.4	11.0
Formic Acid 170 °C	61	49.8 ± 0.1	5.7 ± 0.2	2.6 ± 0.0	0.2 ± 0.0	29.0 ± 0.9	12.7
Formic Acid 200 °C	58	50.8 ± 0.2	5.0 ± 0.1	2.3 ± 0.1	0.2 ± 0.0	27.1 ± 0.3	14.6
Formic Acid 250 °C	44	56.0 ± 1.4	5.1 ± 0.1	2.9 ± 0.1	0.3 ± 0.0	14.9 ± 0.3	20.8
Sulphuric Acid 120 °C	75	47.9 ± 0.5	5.6 ± 0.0	2.2 ± 0.0	1.0 ± 0.0	35.2 ± 2.3	8.1
Sulphuric Acid 170 °C	58	50.5 ± 0.6	5.7 ± 0.0	2.4 ± 0.1	1.7 ± 0.1	29.8 ± 0.7	10.0
Sulphuric Acid 200 °C	57	52.4 ± 0.2	5.5 ± 0.0	2.2 ± 0.0	1.7 ± 0.0	28.1 ± 0.2	10.1
Sulphuric Acid 250 °C	47	56.4 ± 0.7	5.0 ± 0.1	2.7 ± 0.0	3.4 ± 0.0	17.3 ± 0.3	15.1

Table 3. Ultimate analysis proximate analysis and yields of fuels on a dry ash free basis.

Sample Name	Dry Ash Free Basis									
	Yield (%)	C (wt.%)	H (wt.%)	N (wt.%)	S (wt.%)	O (wt.%)	H/C	O/C	Volatile Matter (%)	Fixed Matter (%)
Unprocessed Pig Manure	n/a	50.1	5.8	3.3	0.2	40.6	1.39	0.61	74	26
Sodium Hydroxide 120 °C	84	48.9	5.7	2.8	0.2	42.5	1.40	0.65	80	20
Sodium Hydroxide 170 °C	62	53.0	6.0	2.4	0.1	38.4	1.36	0.54	80	20
Sodium Hydroxide 200 °C	57	57.7	6.2	2.8	0.2	33.1	1.29	0.43	77	23
Sodium Hydroxide 250 °C	34	68.8	6.6	3.4	0.4	20.8	1.15	0.23	68	32
Water 120 °C	88	50.9	6.5	2.7	0.2	39.7	1.53	0.59	82	18
Water 170 °C	61	54.9	5.9	2.7	0.3	36.2	1.28	0.49	78	22
Water 200 °C	58	59.3	6.1	2.8	0.3	31.5	1.24	0.40	76	24
Water 250 °C	38	68.5	6.2	3.6	0.4	21.3	1.09	0.23	67	33
Acetic Acid 120 °C	85	50.5	5.8	2.9	0.2	40.7	1.37	0.60	80	20
Acetic Acid 170 °C	61	55.1	6.0	2.9	0.2	35.8	1.30	0.49	79	21
Acetic Acid 200 °C	58	58.6	5.9	2.7	0.2	32.7	1.21	0.42	75	25
Acetic Acid 250 °C	40	70.5	6.5	3.7	0.3	19.1	1.10	0.20	67	33
Formic Acid 120 °C	85	50.6	6.0	2.8	0.2	40.4	1.43	0.60	81	19
Formic Acid 170 °C	61	57.0	6.5	3.0	0.2	33.2	1.38	0.44	79	21
Formic Acid 200 °C	57	59.5	5.9	2.6	0.2	31.7	1.19	0.40	75	25
Formic Acid 250 °C	40	70.7	6.5	3.6	0.3	18.9	1.10	0.20	68	32
Sulphuric Acid 120 °C	79	52.1	6.1	2.4	1.1	38.3	1.40	0.55	83	17
Sulphuric Acid 170 °C	60	56.1	6.3	2.6	1.9	33.1	1.35	0.44	83	17
Sulphuric Acid 200 °C	59	58.3	6.1	2.4	1.9	31.3	1.26	0.40	76	24
Sulphuric Acid 250 °C	46	66.4	5.9	3.2	4.0	20.4	1.07	0.23	66	34

A van Krevelen plot of the bio-coals from different pH and temperatures is presented in Figure 1. The results indicate that, with increasing temperature, the bio-coal has a more coal-like property, indicating increasing levels of dehydration with increasing temperature and decreasing pH. The pH appears to have a significant influence on dehydration, particularly at lower temperatures (120–170 °C), with sulphuric acid (pH 1) promoting the greatest levels of dehydration and sodium hydroxide (pH 13) showing the least dehydration. This effect of pH on dehydration, however, becomes less as the temperature is increased.

**Figure 1.** Van Krevelen plot of the bio-coals from different pH and temperature.

It should also be noted that the most dehydrated/coalified fuel for the 250 °C treatment is actually formic acid, followed by acetic acid (pH 2.38 and 2.88, respectively). The dry ash free ultimate analysis data presented in Table 3 also indicate that these two acid-treated bio-coals have the highest carbon density with 71% (daf). This higher carbon content could, however, be due to formic and acetic acid adding to the carbon in the bio-coal, lowering the O/C ratio. The use of a mineral acid at pH 2.38 and 2.88 could give an O/C ratio similar to that of water in Table 3 and Figure 1. This is because temperatures

above 200 °C bring about high dissociation of H^+ and OH^- in the water, leading to the decomposition of monosaccharides to organic acids, rapidly dropping process water pH to approximately 3 [37,38]. The results in Table 3 suggest that the bio-coal from sulphuric acid at 250 °C has the lowest carbon content at 66% (daf). It should, however, be noted that the sulphuric acid samples acquired sulphur from the acid, which makes up 4% (daf) of the fuel, while the other samples are low in sulphur; this would reduce the relative carbon content of the fuel when compared to the other treatments, even when correcting to a dry ash free basis. The analysis of the 250 °C bio-coals in Table 3 would suggest that the bio-coal is similar in property to lignite A coal, as described in Smith et al. [39], for all pH treatments.

When the yields are corrected on a dry ash free basis, as shown in Table 3, it indicates that decreasing pH increases yields at 250 °C but decreases yields below 200 °C. This is likely due to the lower pH enhancing the rate of hydrolysis. The generation of hydronium ions due to the presence of acids is known to catalyse the hydrolysis of hemi-cellulose and cellulose into monosaccharides in lignocellulosic biomass [40].

Figure 2 shows the combustion profiles of the bio-coals following different treatments with different pH and temperature, and it shows a distinct volatile burn peak at around 300 °C, which is normally consistent with the presence of cellulose within a fuel [29,30]. Following HTC at 250 °C, this peak is absent, suggesting that the cellulose was removed. The lower yields associated with lower pH in the 120 °C, 170 °C, and 200 °C treatments are due to hydrolysis of the cellulose or “cellulose-like” component within the feedstock, resulting in its removal from the resulting bio-coal. For the 250 °C treatment, the increased yield at lower pH would suggest that pH is catalysing repolymerisation.

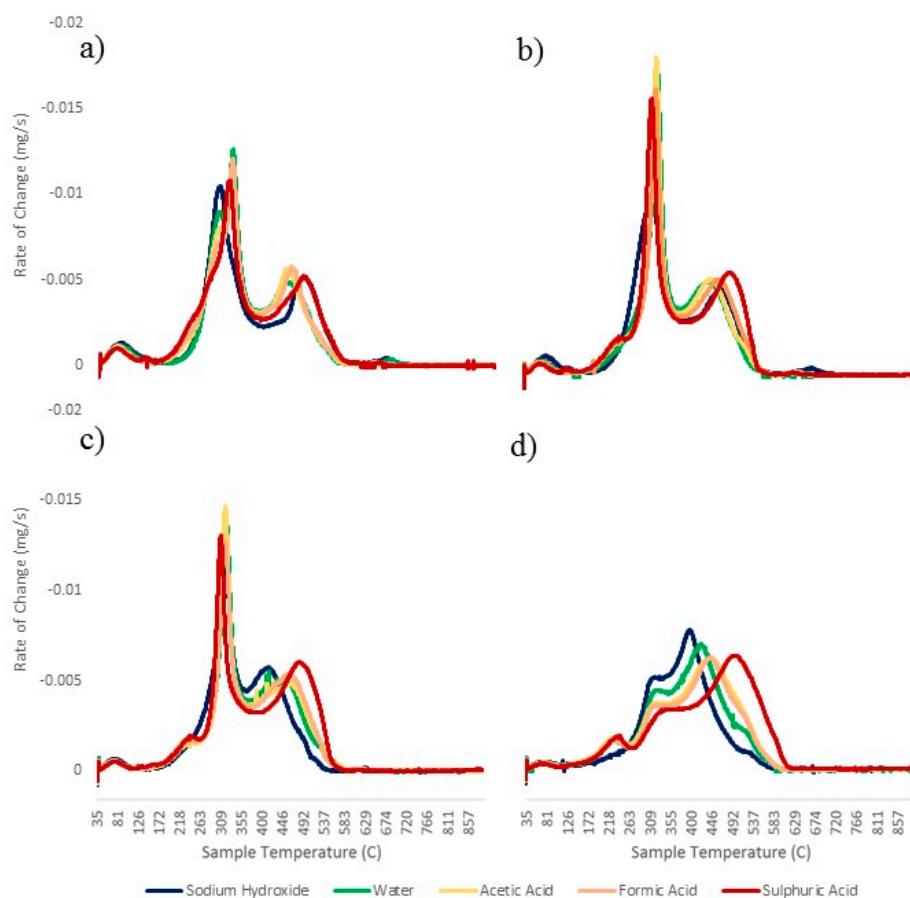


Figure 2. Derivative thermogravimetric (DTG) burning profiles for (a) 120 °C, (b) 170 °C, (c) 200 °C, and (d) 250 °C treatments.

In HTC, the hydrolysis of components such as hemi-cellulose and cellulose results in the formation of monosaccharides within the process water, which then undergo dehydration and fragmentation processes, giving rise to different soluble products such as furfural and hydroxymethylfurfural (HMF), benzenetrol, carboxylic acids, and aldehydes (acetaldehyde, acetonitrilacetone) [40,41]. These decomposition products undergo polymerisation and condensation to form insoluble polymers, often known as humins, which make up a portion of the bio-coal [42,43]. The pH should play a key role in this polymerisation due to the influence pH has on the zeta potential. Zeta potential, or, as it is more correctly known, electrokinetic potential, is a key indicator of the stability of colloidal dispersions, and the magnitude of the zeta potential indicates the degree of repulsion of like-charged particles in that dispersion. A high zeta potential will result in the solution or dispersion resisting agglomeration and flocculation. Bio-coals have a negative zeta potential. This is because they have oxygenated functional groups on their surface, making them behave like weak acids [44]. When a base is added to a suspension with a negative zeta potential, the particles tend to acquire a more negative charge; this reduces the chance of the suspension flocculating and, in the case of hydrothermal suspensions, polymerising to form bio-coal [44]. This is demonstrated in the sodium hydroxide 250 °C bio-coal, which has the lowest yield. If an acid is added to the suspension, a point is reached where the negative charge is neutralised [45]. At this point, the zeta potential is at zero, and it is called the isoelectric point. At this moment, the suspension is most likely to flocculate. For the water- and acid-treated samples, the lower pH increases the yields for the 250 °C treatments, which would suggest that lowering pH reduces the electrokinetic potential of the decomposition products within the aqueous phase, enabling them to polymerise and increase char yield.

The hypothesis that lower pH catalyses flocculation and polymerisation would also support the findings of Ghanim et al. [15], who performed HTC of poultry litter at 250 °C for 2 h using various initial pH with sulphuric acid and found that increasing sulphuric acid content increased bio-coal yield and decreased ash content. This, however, does not agree with the findings in Chen et al. [46], who used sulphuric acid and bagasse and found the reverse. Shorter retention times were, however, used in Chen et al. [46] (5 min, 15 min, and 30 min) and, while the samples underwent polymerisation in Ghanim et al. [15], the extent of repolymerisation was less in Chen et al. [46], as repolymerisation and aromatisation are considerably slower than hydrolysis, decarboxylation, and dehydration reactions which initially occur [3].

When looking at the bulk properties, excluding sulphur content (carbon, hydrogen, nitrogen, oxygen, fixed carbon, and volatile carbon), there is only limited difference between the compositions of the bio-coals produced at 250 °C. This would suggest that, under these conditions, temperature is a more important parameter than pH. The bio-coals produced using the addition of formic and acetic acid result in an increased carbon content in the bio-coal; however, this could be due to the addition of carbon in the form of organic acid, as opposed to an influence of pH. A major increase in sulphur content (4%) is observed in the bio-coal produced using sulphuric acid, indicating incorporation of sulphur, most likely through Maillard chemistry [47].

3.2. Influence of pH on Fuel Inorganic Chemistry

The metal analysis of the bio-coals and unprocessed pig manure is given in Table 4. The results show that, despite apparent increases in ash content, the overall composition of mineral matter in the bio-coal changes depending on the temperature and the pH. For all treatments, most of the potassium, sodium, and strontium is removed into the aqueous phase. The 120 °C treatment with water demonstrates that, for all three metals, around 11% of the original metal is retained within the char, with the remaining 10% gradually reducing with increasing temperature and almost complete removal at 250 °C, regardless of pH. The exception is for the sodium hydroxide treatment, where, at 120 °C, additional sodium is added from the solution. This sodium addition, however, diminishes as the temperature increases and, by the 250 °C treatment, the bio-coal has the equivalent of only 12% of the original sodium in the feedstock along with almost complete removal of the potassium.

Table 4. Main inorganics present within the unprocessed pig manure and derived bio-coals; n/d—not determined.

Sample Name	mg/kg Fuel (db)											
	Na	K	Mg	Ca	Al	Si	P	Mn	Fe	Cu	Zn	Sr
Unprocessed Pig Manure	1426	12,100	9395	27,035	434	3654	15,197	314	1090	140	634	367
Sodium Hydroxide 120 °C	2933	4126	9869	30,212	413	3447	15,431	445	1278	153	604	39
Sodium Hydroxide 170 °C	2020	2927	10,002	41,385	620	4067	19,254	633	1712	230	864	61
Sodium Hydroxide 200 °C	1121	1371	7056	45,915	715	3324	24,748	531	1797	254	963	51
Sodium Hydroxide 250 °C	404	577	17,221	74,240	1174	10,311	41,254	819	3177	394	1771	93
Water 120 °C	193	1493	6232	31,645	546	3710	13,139	411	1464	195	701	45
Water 170 °C	92	1043	5388	41,790	674	3249	21,806	599	1632	227	788	61
Water 200 °C	156	411	6544	38,053	660	3203	25,178	452	1224	197	657	40
Water 250 °C	n/d	392	10,323	61,727	1008	4533	36,468	766	2287	380	1444	80
Acetic Acid 120 °C	199	1920	4201	30,840	572	4709	15,020	433	1447	220	701	45
Acetic Acid 170 °C	37	469	4201	38,345	783	3699	20,876	499	1527	262	758	45
Acetic Acid 200 °C	105	425	4596	43,490	721	3321	23,494	573	1555	271	853	55
Acetic Acid 250 °C	53	397	7123	57,455	941	3504	34,106	590	2252	324	1489	71
Formic Acid 120 °C	114	1048	3685	30,815	576	5344	15,808	403	1523	208	653	42
Formic Acid 170 °C	85	644	3624	37,304	750	3995	20,297	462	1336	234	642	48
Formic Acid 200 °C	125	508	4542	43,529	809	3646	24,236	500	1411	286	803	55
Formic Acid 250 °C	161	743	8307	60,023	1023	4893	34,543	901	2528	317	1516	89
Sulphuric Acid 120 °C	171	1312	1490	19,342	609	5182	2566	56	518	195	234	27
Sulphuric Acid 170 °C	160	1252	1170	25,280	670	4559	1728	n/d	593	222	226	28
Sulphuric Acid 200 °C	125	1213	2152	24,507	709	4287	3815	138	734	203	281	32
Sulphuric Acid 250 °C	28	406	4083	34,688	877	3472	6670	414	1295	336	923	55

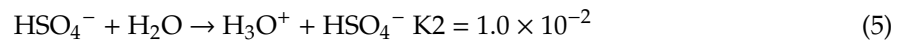
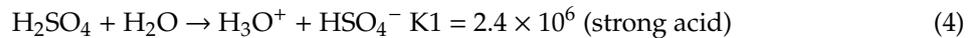
The results of the 120 °C treatment with water are significant, as autoclaving fuel samples at 120 °C for one hour in water is a method provided in BS EN ISO 16995-2 as a methodology for determining free ionic salts within a biofuel. Consequently, metals removed in this treatment can, under BS EN ISO 16995-2, be regarded as in free ionic form. This result would suggest that around 90% of the sodium, potassium, and strontium is in free ionic form within the pig manure, along with 40% of the magnesium and 25% of the phosphorus. The calcium, aluminium, silicon, manganese, iron, copper, and zinc do not appear to be in a water-soluble ionic form. In higher plants, typically over 90% of potassium and sodium is in ionic form, while 60–90% and 30–85% of magnesium and calcium is ionic [48]. The results for the 120 °C treatment with water would suggest that, for pig manure, there is a similar proportion of free ionic potassium and sodium in the fuel, but a greater proportion of the calcium, magnesium, and phosphorus is either organically associated or present in mineral form than in lignocellulosic biomass [16,49]. The relatively low extraction of phosphorus in water at 120 °C would suggest that phosphorus is present as low-solubility salts such as calcium and magnesium phosphate.

The behaviour of silicon is particularly notable in the results as, for all pH treatments, it appears to undergo increasing removal with increasing temperature, with between 45% and 60% retained, depending on pH, at 250 °C. In previous work, it was generally found that silicon is reasonably recalcitrant, being largely retained in the bio-coal, as, to become water-soluble silicon, it has to be hydrated and become silicic acid (H_4O_4Si), which, unless kept buffered within certain boundaries, readily degrades back to insoluble silicon dioxide (SiO_2) [29]. Magnesium retention appears to be strongly influenced by pH, with the highest retentions seen with the sodium hydroxide (pH 13) and reduced retention with decreasing pH. Temperature is also critical, with the highest removal of magnesium typically being observed at 170 °C and increasing retention at 200 °C and 250 °C at all pH.

The metal retention behaviour for magnesium, whereby there is an initial reduction in metal retention up to 170 °C followed by increased retention of metals with increasing temperature between 200 °C and 250 °C, is also observed for calcium, magnesium, iron, and zinc, along with phosphorus. For these elements, there appears to be almost complete retention within the bio-coal at 250 °C for the sodium hydroxide, water, acetic acid, and formic acid treatments. The exception is sulphuric acid, which extracts 50% of the calcium between 120 °C and 200 °C, with 60% retained at 250 °C. Most of the phosphorus is extracted by the sulphuric acid with 87% extracted at 120 °C and 200 °C and over 90% extracted at 170 °C. Additionally, 80% of the original phosphorus is extracted at 250 °C, leaving 20% of the original phosphorus within the bio-coal. Similar ratios of magnesium are extracted as seen for the phosphorus using sulphuric acid. Aluminium and copper appear to remain within the bio-coal irrespective of temperature and pH.

The additional removal of the metals with the addition of sulphuric acid is due to the high dissociation constant of sulphuric acid, which is a strong acid and forms hydronium ions in two stages, with the initial loss of a hydrogen (Equation (4)) and the subsequent decomposition of the bi-sulphate (Equation (5)). Here, 0.1 molar sulphuric acid gives a pH of 1, but the same pH is possible using the same concentration of other strong mineral acids such as hydrochloric acid, or higher concentrations of weaker acids such as acetic acid which only partially dissociate (hence, pH 2.88 at the same molar concentration). The justification for using acid catalysts in HTC, according to Ekpo et al. [8] and Dai et al. [2,7], is to principally mobilise the phosphorus into the aqueous phase for subsequent recovery. The relatively low extraction of phosphorus in water at 120 °C would suggest that phosphorus is present as low-solubility salts such as calcium and magnesium phosphate. The high concentrations of hydronium ions generated by the sulphuric acid are required for the acid leaching of the phosphorus, with the mechanism for acid leaching of calcium given in Equation (6). With sulphuric acid, the calcium is converted to calcium sulphate (see Equation (7)) liberating the phosphorus as phosphoric acid [50]. Similar phosphorus extraction is possible using hydrochloric acid, although, when leaching iron ores, slightly higher efficiency is observed for sulphuric acid [50]. Greater calcium extraction may be possible using hydrochloric acid, as calcium chloride is more water-soluble than calcium sulphate (745 g/L as opposed to 2.6 g/L at standard temperature and pressure (STP)).

This could explain the higher retention of calcium in the bio-coal when compared with magnesium, calcium, phosphorus, manganese, iron, and zinc, as the process water may be saturated once cooled to room temperature.



3.3. Influence of pH on Fuel Combustion Chemistry

Table 5 gives the energy content, the volatile content, and the results of slagging and fouling indices derived from the inorganic chemistry are given in Table 4. The results show that the reaction temperature has the biggest impact on the energy content of the fuel, irrespective of the pH. The results indicate that HTC with sodium hydroxide gives the lowest energy density at all temperatures, and that undertaking HTC in the presence of acids at decreasing pH increases the HHV of the bio-coal, as demonstrated in Ghanim et al. [15]. The highest HHV is observed for acetic and formic acid due to their higher carbon contents, due to the increased carbon within the hydrothermal reaction, as previously discussed; however, there still appears a trend of increasing HHV with decreasing pH.

Table 5. Energy content, volatile content, and slagging and fouling indices for the bio-coals. HHV—higher heating value.

Sample Name	Dry Basis					
	HHV (MJ/kg)	Volatile Matter (%)	Fixed Matter (%)	AI	BAI	$R \frac{b}{a}$
Unprocessed Pig Manure	15.8	64.8	22.6	1.17	0.08	8.54
Sodium Hydroxide 120 °C	14.9	70.9	18.1	0.86	0.14	9.05
Sodium Hydroxide 170 °C	16.7	67.9	16.7	0.54	0.27	8.76
Sodium Hydroxide 200 °C	18.9	62.8	18.8	0.25	0.55	9.91
Sodium Hydroxide 250 °C	21.0	48.3	22.4	0.09	2.55	5.76
Water 120 °C	17.3	76.9	16.9	0.13	0.90	6.63
Water 170 °C	17.6	68.3	18.9	0.09	1.55	8.73
Water 200 °C	19.8	65.7	20.3	0.05	1.92	8.31
Water 250 °C	22.1	54.0	27.0	0.02	6.92	9.32
Acetic Acid 120 °C	16.1	69.9	17.1	0.18	0.73	4.97
Acetic Acid 170 °C	18.1	67.3	17.8	0.04	3.29	6.81
Acetic Acid 200 °C	19.2	63.2	21.0	0.04	2.80	8.52
Acetic Acid 250 °C	23.8	53.4	26.2	0.03	5.19	10.44
Formic Acid 120 °C	16.5	73.5	16.9	0.10	1.39	4.27
Formic Acid 170 °C	19.8	69.3	18.1	0.05	1.90	6.19
Formic Acid 200 °C	19.6	63.4	21.1	0.05	2.12	7.72
Formic Acid 250 °C	23.6	55.4	25.8	0.06	2.72	8.35
Sulphuric Acid 120 °C	17.9	77.7	16.4	0.11	0.36	2.66
Sulphuric Acid 170 °C	19.8	74.3	14.8	0.10	0.44	3.67
Sulphuric Acid 200 °C	20.6	66.7	20.9	0.09	0.58	3.91
Sulphuric Acid 250 °C	23.2	56.3	28.7	0.02	3.28	6.41

The volatile matter content of the bio-coal is also given in Table 5. The volatile matter content is important for predicting combustion behaviour, as, during combustion, the volatiles prevent oxygen from oxidising the carbon, hydrogen, and sulphur present within the fuel particle, bringing about two-stage combustion within a furnace [51]. Moreover, the escaping volatiles burn much more quickly than the char (the fraction remaining after devolatilisation); therefore, understanding the devolatilisation behaviour of a fuel is important in terms of flame ignition, flame stability, flammability limits, and the formation of pollutants such as nitrogen oxides [52]. The volatile content is also useful when determining the equivalent coal rank, with coals with higher ranks having lower volatile contents.

The volatile content appears to be most strongly influenced by reaction temperature, with lower volatile content with increasing reaction temperature. Figure 2 shows the combustion profiles of the bio-coals following different treatments, with the 120 °C, 170 °C, and 200 °C treatments giving a distinct volatile burn peak at around 300 °C. By the 250 °C treatments, this peak is all but removed from the profiles of all fuel. For lignocellulosic biomass combustion, the volatile burn is often closely associated with the thermal decomposition of the hemi-cellulose and cellulose [53,54]. Hemi-cellulose and cellulose are readily degraded at hydrothermal temperatures of 180 °C and 200 °C, respectively [55], and the distinct volatile burn peak at around 300 °C is normally consistent with the presence of cellulose within a fuel [29,30]. This would then suggest the presence, and removal, of fibrous material within the pig manure in a similar manor to that seen for lignocellulosic biomass.

The results presented in Ghanim et al. [15] stated that low pH with sulphuric acid brought higher volatile matter contents in the bio-coal; however, this contradicts the findings in Chen et al. [46], who used sulphuric acid and bagasse and found the inverse. The volatile contents presented in Table 5 would initially support the findings of Ghanim et al. [15]; however, the reason that the volatile matter appears to increase is due to the decrease in ash content of the fuel, increasing the relative amount of volatile matter present. Due to the variation between ash contents with differing pH, the volatile contents are calculated on a dry ash free basis in Table 3 to enable direct comparisons between the volatile chemistry of the different treatments. These results show there is little change between pH, perhaps even suggesting a small decrease in the volatile matter content of the 250 °C treatments with decreasing pH. In the work presented in Chen et al. [46], the fuel was considerably lower in ash than the samples used in Ghanim et al. [15]; thus, there would not be the apparent increase due to the decrease in ash content of the fuel. Consequently, the results presented here would support the findings of both studies.

Combustion of these HTC bio-coals is considered as a coal substitute for coal-powered power plants, enabling utilisation of pre-existing infrastructure. Coal-powered power plants are usually designed to burn a specific type of coal, normally a coal obtained in and around the locality of the plant. Consequently, power stations have a design fuel specification that sets out, amongst others, the ash content, energy content, particle size, and slagging and fouling properties of the fuel. When changing from a design fuel specification, care is required to ensure that the new fuel achieves a stable flame, required to ensure safe boiler operation [56]. Biomass often has different combustion characteristics to that of coal, principally due to a higher proportion of volatile carbon and a much smaller char fraction than those seen in coals [57]. When burning high volatile fuels, combustion starts with the ignition of volatile gases surrounding the fuel particle and prevents oxygen from reaching and igniting the char, resulting in a two-phase combustion called homogeneous ignition, whereas, for typical coals used in pulverised fuel applications, devolatilisation, ignition, and combustion of the volatiles and char combustion occur almost simultaneously [58]. Issues with two-phase combustion occur when you start getting two areas of burning within the furnace that can then draw the flame from the burner and higher in the furnace, bringing about flame instability [52]. This can be a particular issue when co-firing biomass fuels with coal or two fuels with different burning characteristics, as mismatched burning characteristics can result in two fuels burning independently within a furnace. In this instance, the rate of burning (flame velocity) may not match the rate of material feed, leading to the flame either blowing out or flashing back [56]. Thermogravimetric analysis (TGA) is one method originally developed to compare and evaluate fuel burning characteristics using the first derivative thermogravimetric (DTG) curve [52]. When undertaking this test, five key characteristic temperatures are taken, which were developed from the Babcock and Wilcox TGA method for coal and adapted to biomass. The first temperature is the volatile initiation temperature, where the weight loss begins. The second temperature is peak volatile burn, where you get the highest rate of mass loss during devolatilisation. The third temperature is the char initiation temperature, where the rate of combustion changes due to the onset of char combustion. The fourth temperature is peak char burn temperature. The fifth temperature is the burn-out temperature where the weight is constant, indicating the completion of combustion [52].

Figure 2 shows the DTG combustion profiles of the bio-coals following different treatments. For the 120 °C treatment, the acids reduce the first initiation temperature, with weight loss starting at 160 °C for the three acid treatments but 200 °C for the water and alkali treatment. For the water, acetic acid, and formic acid treatments, there appears to be an initial peak at 300 °C, which can be constant with the presence of a fibrous component, such as hemi-cellulose, followed by a larger second peak at 325 °C, which is typically associated with cellulose in lignocellulosic biomass [29,30]. This peak is the peak volatile burn. For the sulphuric acid 120 °C sample, there does not appear to be a distinct peak where the “hemi-cellulose-like” material decomposes, but the presence of a shoulder at 300 °C. A higher mass loss is observed between 160 °C and 300 °C than any other sample, which may suggest that this component is still present but partially hydrolysed, resulting in it thermally decomposing earlier. The sodium hydroxide treatment has only one distinct volatile peak, peaking at about 300 °C. This result is most likely a consequence of the strong basic conditions degrading the “hemi-cellulose-like” material observed with the strong acid conditions, but the high sodium and potassium contents of the fuel (see Table 4) could also be catalysing the volatile burn, giving a different combustion profile [59]. Both the sodium hydroxide and the sulphuric acid treatments have higher char burn temperatures with temperatures of 500 °C, as opposed to 450 °C for the other treatments. The burnout temperature is similar at 580 °C for all treatments.

As the process severity increases, the profiles for 170 °C, 200 °C, and 250 °C retain the first initiation temperature of 160 °C, and a new initial peak begins to arise at 235 °C for the water and acids, initially starting in the 170 °C profile but becoming increasingly pronounced in the 250 °C profile. This peak represents potentially hydrolysed or repolymerised structures chemisorbed to oxygen functional groups on the char surface, yet to dehydrate to form the stable ether or pyrone functional groups required to fix the carbon in the fixed carbon [41]. This peak does not appear in the sodium hydroxide profiles, which has a different combustion profile to that of the water and acid samples, particularly with regard to the volatile burn in the 170 °C and 200 °C profiles, potentially due to the influence of sodium (alkali metals) on catalysing devolatilisation and combustion [59–61]. For all the 170 °C and 200 °C combustion profiles, the main volatile peak becomes increasingly dominant at 325 °C, although, upon reducing its dominance in the 200 °C profiles, the volatile content within the fuel decreases and the fixed matter increases (see Table 5). The increasing dominance of this peak is most likely due to the removal of hydroxyl, carboxyl, and carbonyl groups present within the biomass, along with any structural components that are hydrolysed at lower temperatures such as hemi-cellulose in any cellulosic material present [3,54]. The peak at 325 °C is constant with the presence of residual cellulose and the breaking of its glycosidic linkages [30]. By the 250 °C treatments, the samples adopt a “coal-like” single-stage combustion profile [29], whereby the transition between the volatile release and initiation of char burn (char initiation temperature) is marked more by a “shoulder” as opposed to a distinct peak. This shoulder becomes less distinct with lower pH and correlates with a modest reduction in volatile matter.

The benefit of creating a more “coal-like” burning profile is that it aids flame stability. As previously discussed, when there is a two-stage burn, as seen in the burning profiles for the 120 °C treatments in Figure 2, you get homogeneous combustion, whereby the volatile burn and char burn occur in isolation. In this case, upon drying and devolatilisation, the fuel particle can become entrained in the gas stream and move higher in the furnace while still burning, drawing the flame upward and promoting flame instability [52]. With the single-stage “coal-like” profiles seen in the 250 °C treatments in Figure 2, the devolatilisation, ignition, and combustion of the volatiles do not occur in isolation; instead, the char should oxidise/combust at the same time (heterogeneous reaction), promoting a simultaneous combustion of the fuel mass and a stable flame [57].

In all the profiles, with increasing reaction severity, lower pH increases char burnout temperature. This is particularly notable at 250 °C as the peak temperature (char burn) increases from 400 °C for the sodium hydroxide (pH 13) to 500 °C for the sulphuric acid (pH 1). This result would suggest that pH influences reactivity of the char. There is strong consensus in the literature that the alkali

metals, potassium and sodium, catalyse char reactivity [59,60,62,63], although the concentrations of alkali metals appears similar for the 250 °C bio-coals (see Table 4). The alkaline earth metals, calcium and magnesium, are understood to catalyse char reactivity but to a lesser extent than the alkali metals [63–65], with iron known to behave using similar mechanisms [66]. Given that pH appears to more strongly influence alkaline earth metal content, with higher calcium and magnesium contents, along with iron, associated with higher pH (see Table 4), it is possible that the higher concentrations at higher pH catalyse the thermal decomposition.

Figure 3 displays the ash transition temperatures obtained from the ash fusion test for the four different temperatures and five different pH values. Table 6 gives the transition temperatures for all samples, along with the unprocessed sample, and their standard errors. The results suggest that the unprocessed swine manure has a reasonably high deformation temperature of 1320 °C, compared to between 980 °C and 1140 °C for the conventional *Miscanthus* [26,29]. Despite this result, the shagging and fouling indices suggest almost certain flagging and fouling for these samples. The results of the ash fusion test certainly would suggest a low slagging fuel, possibly due to the high calcium and phosphorus content of the fuel. This would strongly suggest that calcium potassium phosphate complexes and calcium sodium phosphate complexes remove the potassium and sodium available to form low-melting-temperature potassium and sodium silicates [31,32]. A high ash melting temperature is usually indicative of a low alkali metal content and, thus, low fouling propensity temperatures [16], although caution is required here. The results of the 120 °C treatment with water would suggest that around 90% of the sodium and potassium in the fuel is in the form of free ionic salts. Potassium and sodium, when in the form of free ionic salts, are more readily released into the vapour phase and likely to bring about issues with fouling [16,67,68]. The high calcium and phosphorus content of the fuel may, however, prevent this release, instead forming the stable calcium potassium phosphate complexes and calcium sodium phosphate complexes [69]. The slagging and fouling indices used in this paper would not consider such mechanisms when predicting the fuel propensity to slag and foul.

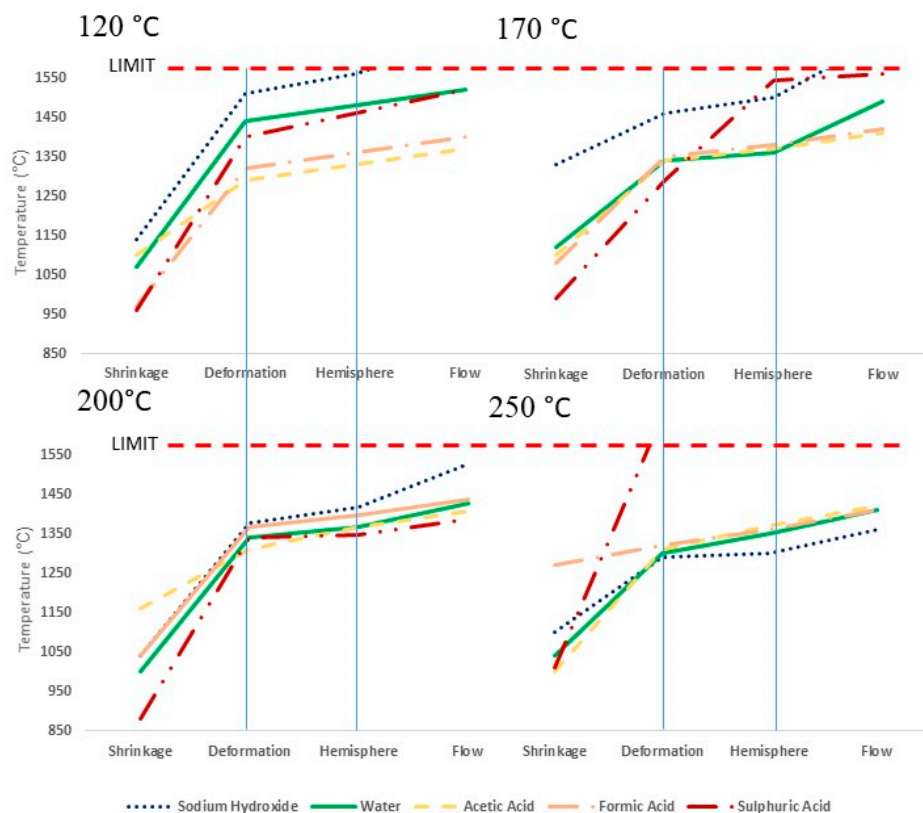


Figure 3. Ash transition temperatures from the ash fusion test for the different treatments at differing hydrothermal treatment temperatures.

Table 6. Ash transition temperatures from the ash fusion test.

Sample Name	Ash Transition Temperature (°C)			
	Shrinkage	Deformation	Hemisphere	Flow
Unprocessed	1260 ± 0	1320 ± 0	1380 ± 0	1500 ± 0
Sodium Hydroxide 120 °C	1140 ± 0	1510 ± 0	1560 ± 10	>1570
Sodium Hydroxide 170 °C	1330 ± 0	1460 ± 20	1500 ± 10	>1570
Sodium Hydroxide 200 °C	1040 ± 0	1380 ± 10	1420 ± 0	1530 ± 0
Sodium Hydroxide 250 °C	1100 ± 0	1290 ± 0	1300 ± 0	1360 ± 0
Water 120 °C	1070 ± 0	1440 ± 0	1480 ± 0	1520 ± 0
Water 170 °C	1120 ± 0	1340 ± 0	1360 ± 0	1490 ± 0
Water 200 °C	1000 ± 0	1340 ± 0	1370 ± 0	1430 ± 0
Water 250 °C	1040 ± 0	1300 ± 0	1350 ± 0	1410 ± 0
Acetic Acid 120 °C	1100 ± 0	1290 ± 0	1330 ± 0	1370 ± 0
Acetic Acid 170 °C	1100 ± 0	134 ± 00	1370 ± 0	1410 ± 0
Acetic Acid 200 °C	1160 ± 0	1310 ± 0	1370 ± 0	1410 ± 0
Acetic Acid 250 °C	1000 ± 0	1310 ± 0	1370 ± 0	1420 ± 0
Formic Acid 120 °C	970 ± 0	1320 ± 0	1360 ± 0	1400 ± 0
Formic Acid 170 °C	1080 ± 0	1350 ± 0	1380 ± 0	1420 ± 0
Formic Acid 200 °C	1040 ± 0	1370 ± 0	1400 ± 0	1440 ± 0
Formic Acid 250 °C	1270 ± 0	1320 ± 0	1360 ± 0	1410 ± 0
Sulphuric Acid 120 °C	960 ± 0	1400 ± 80	1460 ± 60	1520 ± 20
Sulphuric Acid 170 °C	990 ± 0	129 ± 00	1545 ± 5	1560 ± 0
Sulphuric Acid 200 °C	880 ± 0	1340 ± 0	1350 ± 0	1390 ± 0
Sulphuric Acid 250 °C	1010 ± 0	>1570		

For the hydrothermally treated samples, the results show that ash shrinkage temperature is reduced; however, this is believed to be due to formation of carbonates during the hydrothermal process [26,28,29]. The deformation and hemisphere temperatures, however, appear to change reasonably little, indicating limited change to slagging propensity. The exception to this is the low-temperature sodium hydroxide-treated samples and the 250 °C treated sulphuric acid sample. The 120 °C, 170 °C, and 200 °C sodium hydroxide samples are suppressing, given that these are the only hydrothermal samples where the alkali index (given in Table 5) suggests almost certain slagging and fouling. Sodium and potassium contents are, however reduced, when compared to the starting feedstock, which may explain this increase.

In the 250 °C treated sulphuric acid sample, there is the greatest improvement in ash behaviour with the sample not undergoing deformation within the test conditions (test limit 1570 °C). This is predominantly due to the ash becoming a highly stable magnesium calcium phosphate silicate complex. It should be noted that the sulphuric acid samples acquire sulphur from the acid, which makes up 3.4% (db) of the fuel. Sulphur can play both a positive and a negative role during combustion in large combustion plants. During combustion, sulphur is predominantly oxidised to sulphur dioxide (SO₂) (>95%), but some sulphur trioxide (SO₃) is also formed [16]. While the sulphur dioxide plays an undesirable role in terms of corrosion, active oxidation of furnace components, and emissions of sulphur dioxide to the atmosphere (unless abated using flue gas desulphurisation) [17], sulphur trioxide plays an important role in the abatement of particulate emissions. This is due to the thermally derived sulphur trioxide forming sulphuric acid in the flue gas, which then adsorbs onto the fly ash particulates [70]. This affects the surface electrical conductivity of the particulate, greatly increasing the efficiency of the electrostatic precipitators [71]. This could be particularly advantageous for the 250 °C treated sulphuric acid sample, given that potential to emit (PTE) metals (strontium, copper, and zinc) are present within the swine manure and the derived hydrothermal fuels. Precipitation of these in the fly ash would be required to avoid issues with emissions.

When combusting fuel in pulverised applications, fuel sulphur is desirable as, while sulphur emissions are largely in the form of sulphur dioxide, when a fuel with high sulphur content is combusted, there is generally enough sulphur trioxide formed to bring the electrical resistivity of the fly ash into a range which results in good precipitator operation [72]. This can be a particular

issue with biomass, which is typically low in sulphur and results in a very low collection efficiency of electrostatic precipitators [72]; consequently, biomass-fuelled furnaces, such as Drax (UK), add sulphur to overcome this. The sulphur content of the 250 °C treated sulphuric acid sample is typically too high for single-fuel combustion; however, if blended with low sulphur biofuels or coal, this sulphur content could be brought within “design fuel” specification. Moreover, the magnesium calcium phosphate silicate ash of the fuel would have an additive influence and could improve the slagging and fouling propensity of the blended biomass and coal. Consequently, with blending, the 250 °C treated sulphuric acid fuel could be safely combusted within the pulverised fuel plant if appropriately blended.

4. Conclusions

The influence of pH most strongly influences ash chemistry, with decreasing pH increasing the removal of ash. This reduction in ash has the biggest influence on the volatile carbon and energy content of the fuel, with lower ash contents bringing about higher energy densities when calculated on a dry basis for a given temperature. The pH also influences dehydration, with fuel dehydration increased with decreasing pH, although, with increasing temperature, the influence pH has on dehydration becomes less. The pH and temperature appear to influence yield, with lower pH increasing yields above 250 °C but decreasing yields below 200 °C. The lower yields below 200 °C appear due to the acids catalysing hydrolysis of “cellulose-like” fibres within the swine manure, whereas the higher yields at 250 °C could be due to the low pH catalysing polymerisation due to its influence on the electrokinetic potential of the hydrothermal suspension.

The water experiments at 120 °C would suggest that around 90% of the sodium and potassium is in free ionic form within the pig manure, along with 40% of the magnesium and 25% of the phosphorus. This free ionic sodium and potassium are more readily released into the vapour phase, and they are likely to bring about issues with fouling if combusted. Slagging and fouling indices suggest that they cannot be safely combusted without treatment. Nonetheless, the ash fusion test suggests reasonably high deformation temperatures, suggesting low slagging and fouling. This paradox is brought about through the high calcium and phosphorus content of the fuel forming the stable calcium potassium/sodium phosphate complexes. Hydrothermally treating the fuels achieves almost complete removal of sodium and potassium and their associated issues with fouling. Increasing reaction temperature appears to immobilise calcium, magnesium, iron, zinc, and phosphorus within the bio-coal unless treated at low pH, which enables mobilisation of the phosphorus and alkaline earth metals. Treatment at 250 °C results in a more coal-like combustion fuel, with fuel properties similar to that of lignite coal and an HHV between 21 and 23 MJ/kg depending on pH. The removal of the alkaline earth metals and iron reduces the reactivity of the fuel treated at pH 1. Despite the mobilisation of calcium and phosphorus using strong acid, sufficient calcium and phosphorus is retained within the ash to give very favourable ash chemistry in terms of slagging and fouling. The use of sulphuric acid does result in residual sulphur within the fuel; however, this sulphur may be beneficial due to the influence that thermally derived sulphur trioxide has on the collection efficiency of electrostatic precipitators and particulate removal, if appropriately blended with another low-sulphur fuel.

Author Contributions: Conceptualisation, A.M.S., U.E., and A.B.R.; methodology, A.M.S.; validation, A.M.S.; formal analysis, A.M.S.; investigation, A.M.S.; resources, A.B.R.; data curation, A.M.S. and U.E.; writing—original draft preparation, A.M.S.; writing—review and editing, A.M.S. and A.B.R.; visualisation, A.M.S.; supervision, A.B.R. All authors have read and agreed to the published version of the manuscript.

Funding: This research was funded by the Engineering and Physical Sciences Research Council (EPSRC) Doctoral Training Centre in Low Carbon Technologies (EP/G036608/1), the Niger Delta Development Commission (NDDC), the European Commission ERDF Interreg IVb NEW “Biorefine” project and Grønt Udviklings- og Demonstrationsprogram (GUDP) (34009-18-1435).

Acknowledgments: The authors would like to thank the University of Leeds farm for the supply of swine manure and would also like to thank Simon Lloyd, Karine Alves Thorne, and Adrian Cunliffe from the University of Leeds for their technical assistance.

Conflicts of Interest: The authors declare no conflicts of interest.

References

1. Szogi, A.A.; Vanotti, M.B.; Ro, K.S. Methods for Treatment of Animal Manures to Reduce Nutrient Pollution Prior to Soil Application. *Curr. Pollut. Rep.* **2015**, *1*, 47–56. [[CrossRef](#)]
2. Heilmann, S.M.; Molde, J.S.; Timler, J.G.; Wood, B.M.; Mikula, A.L.; Vozhdayev, G.V.; Colosky, E.C.; Spokas, K.A.; Valentas, K.J. Phosphorus Reclamation through Hydrothermal Carbonization of Animal Manures. *Environ. Sci. Technol.* **2014**, *48*, 10323–10329. [[CrossRef](#)]
3. Funke, A.; Ziegler, F. Hydrothermal carbonization of biomass: A summary and discussion of chemical mechanisms for process engineering. *Biofuels Bioprod. Biorefining* **2010**, *4*, 160–177. [[CrossRef](#)]
4. Heilmann, S.M.; Davis, H.T.; Jader, L.R.; Lefebvre, P.A.; Sadowsky, M.J.; Schendel, F.J.; von Keitz, M.G.; Valentas, K.J. Hydrothermal carbonization of microalgae. *Biomass Bioenergy* **2010**, *34*, 875–882. [[CrossRef](#)]
5. Heilmann, S.M.; Jader, L.R.; Sadowsky, M.J.; Schendel, F.J.; von Keitz, M.G.; Valentas, K.J. Hydrothermal carbonization of distiller's grains. *Biomass Bioenergy* **2011**, *35*, 2526–2533. [[CrossRef](#)]
6. Ekpo, U.; Ross, A.B.; Camargo-Valero, M.A.; Williams, P.T. A comparison of product yields and inorganic content in process streams following thermal hydrolysis and hydrothermal processing of microalgae, manure and digestate. *Bioresour. Technol.* **2016**, *200*, 951–960. [[CrossRef](#)]
7. Dai, L.; Tan, F.; Wu, B.; He, M.; Wang, W.; Tang, X.; Hu, Q.; Zhang, M. Immobilization of phosphorus in cow manure during hydrothermal carbonization. *J. Environ. Manag.* **2015**, *157*, 49–53. [[CrossRef](#)] [[PubMed](#)]
8. Ekpo, U.; Ross, A.B.; Camargo-Valero, M.A.; Fletcher, L.A. Influence of pH on hydrothermal treatment of swine manure: Impact on extraction of nitrogen and phosphorus in process water. *Bioresour. Technol.* **2016**, *214*, 637–644. [[CrossRef](#)] [[PubMed](#)]
9. Titirici, M.-M.; Thomas, A.; Antonietti, M. Back in the black: hydrothermal carbonization of plant material as an efficient chemical process to treat the CO₂ problem? *New J. Chem.* **2007**, *31*, 787–789. [[CrossRef](#)]
10. Hu, B.; Yu, S.-H.; Wang, K.; Liu, L.; Xu, X.-W. Functional carbonaceous materials from hydrothermal carbonization of biomass: an effective chemical process. *Dalton Trans.* **2008**, 5414–5423. [[CrossRef](#)] [[PubMed](#)]
11. Lu, X.; Zhang, Y.; Angelidaki, I. Optimization of H₂SO₄-catalyzed hydrothermal pretreatment of rapeseed straw for bioconversion to ethanol: focusing on pretreatment at high solids content. *Bioresour. Technol.* **2009**, *100*, 3048–3053. [[CrossRef](#)]
12. Demir-Cakan, R.; Baccile, N.; Antonietti, M.; Titirici, M.-M. Carboxylate-rich carbonaceous materials via one-step hydrothermal carbonization of glucose in the presence of acrylic acid. *Chem. Mater.* **2009**, *21*, 484–490. [[CrossRef](#)]
13. Lynam, J.G.; Coronella, C.J.; Yan, W.; Reza, M.T.; Vasquez, V.R. Acetic acid and lithium chloride effects on hydrothermal carbonization of lignocellulosic biomass. *Bioresour. Technol.* **2011**, *102*, 6192–6199. [[CrossRef](#)] [[PubMed](#)]
14. Reza, M.T.; Rottler, E.; Herklotz, L.; Wirth, B. Hydrothermal carbonization (HTC) of wheat straw: Influence of feedwater pH prepared by acetic acid and potassium hydroxide. *Bioresour. Technol.* **2015**, *182*, 336–344. [[CrossRef](#)] [[PubMed](#)]
15. Ghanim, B.M.; Kwapinski, W.; Leahy, J.J. Hydrothermal carbonisation of poultry litter: Effects of initial pH on yields and chemical properties of hydrochars. *Bioresour. Technol.* **2017**, *238*, 78–85. [[CrossRef](#)] [[PubMed](#)]
16. Koppejan, J.; Van Loo, S. *The Handbook of Biomass Combustion and Co-Firing*; Earthscan: London, UK, 2012.
17. Riedl, R.; Dahl, J.; Obernberger, I.; Narodslawsky, M. Corrosion in fire tube boilers of biomass combustion plants. In Proceedings of the China International Corrosion Control Conference, Beijing, China, 9–13 October 1999.
18. Volpe, M.; Goldfarb, J.L.; Fiori, L. Hydrothermal carbonization of *Opuntia ficus-indica* cladodes: Role of process parameters on hydrochar properties. *Bioresour. Technol.* **2018**, *247*, 310–318. [[CrossRef](#)] [[PubMed](#)]
19. Mäkelä, M.; Kwong, C.W.; Broström, M.; Yoshikawa, K. Hydrothermal treatment of grape marc for solid fuel applications. *Energy Convers. Manag.* **2017**, *145*, 371–377. [[CrossRef](#)]
20. Lane, D.J.; Truong, E.; Larizza, F.; Chiew, P.; de Nys, R.; van Eyk, P.J. Effect of Hydrothermal Carbonization on the Combustion and Gasification Behavior of Agricultural Residues and Macroalgae: Devolatilization Characteristics and Char Reactivity. *Energy Fuels* **2017**. [[CrossRef](#)]

21. Petrovil, J.; Perisil, N.; Maksimovil, J.D.; Maksimovil, V.; Kragovil, M.; Stojanovil, M.; Lauševil, M.; Mihajlović, M. Hydrothermal conversion of grape pomace: Detailed characterization of obtained hydrochar and liquid phase. *J. Anal. Appl. Pyrolysis* **2016**, *118*, 267–277. [[CrossRef](#)]
22. Bach, Q.-V.; Tran, K.-Q.; Skreiberg, Ø. Accelerating wet torrefaction rate and ash removal by carbon dioxide addition. *Fuel Process. Technol.* **2015**, *140*, 297–303. [[CrossRef](#)]
23. Benavente, V.; Calabuig, E.; Fullana, A. Upgrading of moist agro-industrial wastes by hydrothermal carbonization. *J. Anal. Appl. Pyrolysis* **2014**, *113*, 89–98. [[CrossRef](#)]
24. Broch, A.; Jena, U.; Hoekman, S.; Langford, J. Analysis of Solid and Aqueous Phase Products from Hydrothermal Carbonization of Whole and Lipid-Extracted Algae. *Energies* **2013**, *7*, 62. [[CrossRef](#)]
25. Reza, M.T.; Lynam, J.G.; Uddin, M.H.; Coronella, C.J. Hydrothermal carbonization: Fate of inorganics. *Biomass Bioenergy* **2013**, *49*, 86–94. [[CrossRef](#)]
26. Smith, A.M.; Singh, S.; Ross, A.B. Fate of inorganic material during hydrothermal carbonisation of biomass: Influence of feedstock on combustion behaviour of hydrochar. *Fuel* **2016**, *169*, 135–145. [[CrossRef](#)]
27. Mäkelä, M.; Yoshikawa, K. Ash behavior during hydrothermal treatment for solid fuel applications. Part 2: Effects of treatment conditions on industrial waste biomass. *Energy Convers. Manag.* **2016**, *121*, 409–414. [[CrossRef](#)]
28. Smith, A.M.; Ross, A.B. Production of bio-coal, bio-methane and fertilizer from seaweed via hydrothermal carbonisation. *Algal Res.* **2016**, *16*, 1–11. [[CrossRef](#)]
29. Smith, A.M.; Whittaker, C.; Shield, I.; Ross, A.B. The potential for production of high quality bio-coal from early harvested Miscanthus by hydrothermal carbonisation. *Fuel* **2018**, *220*, 546–557. [[CrossRef](#)]
30. Smith, A.M.; Ross, A.B. The Influence of Residence Time during Hydrothermal Carbonisation of Miscanthus on Bio-Coal Combustion Chemistry. *Energies* **2019**, *12*, 523. [[CrossRef](#)]
31. Grimm, A.; Skoglund, N.; Boström, D.; Ohman, M. Bed agglomeration characteristics in fluidized quartz bed combustion of phosphorus-rich biomass fuels. *Energy Fuels* **2011**, *25*, 937–947. [[CrossRef](#)]
32. Lindström, E.; Sandström, M.; Boström, D.; Öhman, M. Slagging Characteristics during Combustion of Cereal Grains Rich in Phosphorus. *Energy Fuels* **2007**, *21*, 710–717. [[CrossRef](#)]
33. Thy, P.; Jenkins, B.M.; Grundvig, S.; Shiraki, R.; Leshner, C.E. High temperature elemental losses and mineralogical changes in common biomass ashes. *Fuel* **2006**, *85*, 783–795. [[CrossRef](#)]
34. Thy, P.; Leshner, C.E.; Jenkins, B.M. Experimental determination of high-temperature elemental losses from biomass slag. *Fuel* **2000**, *79*, 693–700. [[CrossRef](#)]
35. Jenkins, B.; Baxter, L.; Miles, T. Combustion properties of biomass. *Fuel Process. Technol.* **1998**, *54*, 17–46. [[CrossRef](#)]
36. Bapat, D.; Kulkarni, S.; Bhandarkar, V. *Design and Operating Experience on Fluidized Bed Boiler Burning Biomass Fuels with High Alkali Ash*; American Society of Mechanical Engineers: New York, NY, USA, 1997.
37. Antal, M.J.; Mok, W.S.L.; Richards, G.N. Mechanism of formation of 5-(hydroxymethyl)-2-furaldehyde from d-fructose and sucrose. *Carbohydr. Res.* **1990**, *199*, 91–109. [[CrossRef](#)]
38. Jin, F.; Zhou, Z.; Moriya, T.; Kishida, H.; Higashijima, H.; Enomoto, H. Controlling hydrothermal reaction pathways to improve acetic acid production from carbohydrate biomass. *Environ. Sci. Technol.* **2005**, *39*, 1893–1902. [[CrossRef](#)]
39. Smith, K.L.; Smoot, L.D.; Fletcher, T.H.; Pugmire, R.J. *The Structure and Reaction Processes of Coal*; Springer Science & Business Media: New York, NY, USA, 2013.
40. Garrote, G.; Domínguez, H.; Parajó, J.C. Hydrothermal processing of lignocellulosic materials. *Holz als Roh-und Werkst.* **1999**, *57*, 191–202. [[CrossRef](#)]
41. Sevilla, M.; Fuertes, A.B. Chemical and Structural Properties of Carbonaceous Products Obtained by Hydrothermal Carbonization of Saccharides. *Chem. Eur. J.* **2009**, *15*, 4195–4203. [[CrossRef](#)]
42. Kei-ichi, S.; Yoshihisa, I.; Hitoshi, I. Catalytic Activity of Lanthanide(III) Ions for the Dehydration of Hexose to 5-Hydroxymethyl-2-furaldehyde in Water. *Bull. Chem. Soc. Jpn.* **2001**, *74*, 1145–1150. [[CrossRef](#)]
43. Patil, S.K.R.; Lund, C.R.F. Formation and Growth of Humins via Aldol Addition and Condensation during Acid-Catalyzed Conversion of 5-Hydroxymethylfurfural. *Energy Fuels* **2011**, *25*, 4745–4755. [[CrossRef](#)]
44. Baccile, N.; Antonietti, M.; Titirici, M.-M. One-Step Hydrothermal Synthesis of Nitrogen-Doped Nanocarbons: Albumine Directing the Carbonization of Glucose. *ChemSusChem* **2010**, *3*, 246–253. [[CrossRef](#)]
45. Yu, L.; Falco, C.; Weber, J.; White, R.J.; Howe, J.Y.; Titirici, M.-M. Carbohydrate-Derived Hydrothermal Carbons: A Thorough Characterization Study. *Langmuir* **2012**, *28*, 12373–12383. [[CrossRef](#)] [[PubMed](#)]

46. Chen, W.-H.; Ye, S.-C.; Sheen, H.-K. Hydrothermal carbonization of sugarcane bagasse via wet torrefaction in association with microwave heating. *Bioresour. Technol.* **2012**, *118*, 195–203. [[CrossRef](#)] [[PubMed](#)]
47. Wohlgemuth, S.-A.; Vilela, F.; Titirici, M.-M.; Antonietti, M. A one-pot hydrothermal synthesis of tunable dual heteroatom-doped carbon microspheres. *Green Chem.* **2012**, *14*, 741–749. [[CrossRef](#)]
48. Marschner, H.; Marschner, P. *Marschner's Mineral Nutrition of Higher Plants*; Academic Press: Cambridge, MA, USA, 2012.
49. Korbee, R.; Kiel, J.; Zevenhoven, M.; Skrifvars, B.; Jensen, P.; Frandsen, F. Investigation of biomass inorganic matter by advanced fuel analysis and conversion experiments. In *Proceedings of the Power Production in the 21st Century: Impacts of Fuel Quality and Operations*; United Engineering Foundation Advanced Combustion Engineering Research Center: Snowbird, UT, USA, 2001.
50. Jin, Y.-S.; Jiang, T.; Yang, Y.-B.; Li, Q.; Li, G.-H.; Guo, Y.-F. Removal of phosphorus from iron ores by chemical leaching. *J. Cent. South Univ. Technol.* **2006**, *13*, 673–677. [[CrossRef](#)]
51. Miller, B.G.; Tillman, D.A. *Combustion Engineering Issues for Solid Fuel Systems*; Elsevier: Amsterdam, The Netherlands, 2008.
52. Tillman, D.A.; Duong, D.N.B.; Harding, N.S. Chapter 4—Blending Coal with Biomass: Cofiring Biomass with Coal. In *Solid Fuel Blending*; Tillman, D.A., Duong, D.N.B., Harding, N.S., Eds.; Butterworth-Heinemann: Boston, MA, USA, 2012; pp. 125–200. [[CrossRef](#)]
53. Dahlquist, E. *Technologies for Converting Biomass to Useful Energy*, 1st ed.; CRC Press: Boca Raton, FL, USA, 2013.
54. Yang, H.; Yan, R.; Chen, H.; Lee, D.H.; Zheng, C. Characteristics of hemicellulose, cellulose and lignin pyrolysis. *Fuel* **2007**, *86*, 1781–1788. [[CrossRef](#)]
55. Peterson, A.A.; Vogel, F.; Lachance, R.P.; Fröling, M.; Antal, M.J., Jr.; Tester, J.W. Thermochemical biofuel production in hydrothermal media: A review of sub- and supercritical water technologies. *Energy Environ. Sci.* **2008**, *1*, 32–65. [[CrossRef](#)]
56. Su, S.; Pohl, J.H.; Holcombe, D.; Hart, J.A. Techniques to determine ignition, flame stability and burnout of blended coals in p.f. power station boilers. *Prog. Energy Combust. Sci.* **2001**, *27*, 75–98. [[CrossRef](#)]
57. Williams, A.; Jones, J.; Ma, L.; Pourkashanian, M. Pollutants from the combustion of solid biomass fuels. *Prog. Energy Combust. Sci.* **2012**, *38*, 113–137. [[CrossRef](#)]
58. Yarin, L.P.; Hetsroni, G.; Mosyak, A. *Combustion of Two-Phase Reactive Media*; Springer Science & Business Media: Heidelberg, Germany, 2013.
59. Saddawi, A.; Jones, J.M.; Williams, A. Influence of alkali metals on the kinetics of the thermal decomposition of biomass. *Fuel Process. Technol.* **2012**, *104*, 189–197. [[CrossRef](#)]
60. Jones, J.M.; Darvell, L.I.; Pourkashanian, M.; Williams, A. The Role of Metals in Biomass Char Combustion. In *Proceedings of the European Combustion Meeting*, Louvain-la-Neuve, Belgium, 3–6 April 2005.
61. Nowakowski, D.J.; Jones, J.M.; Brydson, R.M.D.; Ross, A.B. Potassium catalysis in the pyrolysis behaviour of short rotation willow coppice. *Fuel* **2007**, *86*, 2389–2402. [[CrossRef](#)]
62. Huang, H.Y.; Yang, R.T. Catalyzed Carbon–NO Reaction Studied by Scanning Tunneling Microscopy and ab Initio Molecular Orbital Calculations. *J. Catal.* **1999**, *185*, 286–296. [[CrossRef](#)]
63. Backreedy, R.I.; Jones, J.M.; Pourkashanian, M.; Williams, A. Burn-out of pulverised coal and biomass chars. *Fuel* **2003**, *82*, 2097–2105. [[CrossRef](#)]
64. Kannan, M.P.; Richards, G.N. Gasification of biomass chars in carbon dioxide: dependence of gasification rate on the indigenous metal content. *Fuel* **1990**, *69*, 747–753. [[CrossRef](#)]
65. Stojanowska, G.; Jones, J. Influence of added calcium on thermal decomposition of biomass, lignite and their blends. *Arch. Combust.* **2006**, *26*, 91.
66. Backreedy, R.I.; Jones, J.M.; Pourkashanian, M.; Williams, A. Modeling the reaction of oxygen with coal and biomass chars. *Proc. Combust. Inst.* **2002**, *29*, 415–421. [[CrossRef](#)]
67. Skrifvars, B.-J.; Laurén, T.; Hupa, M.; Korbee, R.; Ljung, P. Ash behaviour in a pulverized wood fired boiler—A case study. *Fuel* **2004**, *83*, 1371–1379. [[CrossRef](#)]
68. Miles, T.R.; Miles, T., Jr.; Baxter, L.; Bryers, R.; Jenkins, B.; Oden, L. *Alkali Deposits Found in Biomass Power Plants: A preliminary Investigation of Their Extent and Nature*; National Renewable Energy Lab.: Golden, CO, USA; Miles Thomas R.: Portland, OR, USA; Sandia National Labs.: Livermore, CA, USA; Foster Wheeler Development Corp.: Livingston, NJ, USA; California University: Davis, CA, USA; Bureau of Mines, Albany Research Center: Albany, OR, USA, 1995; Volume 1.

69. Wang, L.; Hustad, J.E.; Skreiberg, Ø.; Skjevraak, G.; Grønli, M. A Critical Review on Additives to Reduce Ash Related Operation Problems in Biomass Combustion Applications. *Energy Procedia* **2012**, *20*, 20–29. [[CrossRef](#)]
70. Dahlin, R.S.; Vann Bush, P.; Snyder, T.R. *Fundamental Mechanisms in Flue-Gas Conditioning. Topical Report No. 1, Literature Review and Assembly of Theories on the Interactions of Ash and FGD Sorbents*; Southern Research Inst.: Birmingham, AL, USA, 1992.
71. Parker, K.R. *Applied Electrostatic Precipitation*; Springer Science & Business Media: Dordrecht, The Netherlands, 2012.
72. Shanthakumar, S.; Singh, D.N.; Phadke, R.C. Flue gas conditioning for reducing suspended particulate matter from thermal power stations. *Prog. Energy Combust. Sci.* **2008**, *34*, 685–695. [[CrossRef](#)]



© 2020 by the authors. Licensee MDPI, Basel, Switzerland. This article is an open access article distributed under the terms and conditions of the Creative Commons Attribution (CC BY) license (<http://creativecommons.org/licenses/by/4.0/>).